JOURNAL OF SOLID STATE CHEMISTRY 113, 289–295 (1994)

Preparation, Characterization, and Structure of α-Zirconium Hydrogen Phosphate Hemihydrate

G. Alberti,* U. Costantino,* R. Millini,†,[1] G. Perego,† and R. Vivani*

*Dipartimento di Chimica, Università di Perugia, via Elce di Sotto 8, I-06123 Perugia, Italy; and †Eniricerche S.p.A. via F. Maritano 26, I-20097 San Donato Milanese, Italy

Received November 8, 1993; in revised form February 18, 1994; accepted February 23, 1994

A hemihydrate form of layered zirconium phosphate was obtained by reacting ZrO_2 with concentrated H_3PO_4 (17 *M*) at 230°C for 2 days. $Zr(HPO_4)_2 \cdot 0.5H_2O$ crystallizes in the monoclinic symmetry with cell constants $a = 9.1478(5)$ Å, $b = 5.3242(3)$ Å, $c = 15.288(1)$ Å, $\beta = 103.848(6)°$, space group $C2/c$. It undergoes a reversible phase transition at about 70°C, without losing the lattice water; the interlayer distance is reduced to 7.30 Å and the symmetry changes to the trigonal one ($a = 5.3743(5)$ Å, $c = 21.982(2)$ Å, space group $R\bar{3}$). The crystal structure of the hemihydrate phase at room temperature was determined by using 36 unambiguously indexed reflections, obtained by the decomposition of the X-ray diffraction pattern, in a conventional single-crystal analysis. A geometric model was assumed for the high-temperature phase. Refinement of the crystal structures was performed by the Rietveld method. In the low-temperature phase, the crystallization water forms interlayer hydrogen bonds with the P–OH of the α-layers, which accounts for the very long times or the elevated temperature required for complete dehydration to occur. Accordingly, the hemihydrate does not transform into the monohydrate phase even when dipped into boiling water and it does not seem obtainable from partial dehydration of the monohydrate form. © 1994 Academic Press, Inc.

INTRODUCTION

Since the pioneering studies of Clearfield and Stynes (1) and Alberti and Torracca (2), many layered phosphates and arsenates of tetravalent metals have been synthesized and characterized. Two different structure types of the layers, usually referred to as α and γ (3–5), exist and a large number of phases can be obtained by the partial or total exchange of the protons of the α- or γ-layers with other cations, as well as by the intercalation of polar molecules (H_2O, NH_3, alcohols, amines, etc.) in the interlayer region. Moreover, many organic derivatives of both α- and γ-zirconium phosphate have been synthesized (6, 7).

[1] To whom correspondence should be addressed.

Many of the compounds prepared are of interest for practical applications in ion exchange, intercalation, ionic (in particular protonic) conductivity, heterogeneous catalysis, and ionic and molecular sieving. They have, therefore, been intensively studied and hundreds of papers and patents have been published. The interested reader is referred to some recent reviews and books (8–12). Despite much research activity, some basic aspects concerning the crystallochemistry of the $Zr(IV)/H_3PO_4$ system are, as yet, not fully elucidated. When zirconium phosphate gels are refluxed in highly concentrated phosphoric acid for a long time, phases different from the typical α-$Zr(HPO_4)_2 \cdot H_2O$ are obtained (13), very likely by a mechanism of solubilization–crystallization of the gel (14). Furthermore, zirconium phosphates having a P/Zr molar ratio higher than 2 are formed after the dissolution of $ZrOCl_2$ in pure H_3PO_4 at 80–200°C (15). The stoichiometry and crystal structure of these compounds are not well known; moreover, their preparation procedure needs to be better defined.

During a systematic study of the $Zr(IV)/H_3PO_4$ system, a new layered compound with the formula $Zr(HPO_4)_2 \cdot 0.5H_2O$, characterized by an interlayer distance of 7.42 Å, was isolated. The synthesis, the main properties, and the crystal structure of this phase are reported and discussed.

EXPERIMENTAL

Reagents

All reagents were C.Erba R.P.E. α-$Zr(HPO_4)_2 \cdot H_2O$ was prepared according to the direct precipitation method (2).

Preparation Procedures

The syntheses were carried out in sealed vessels under shaking, at a controlled temperature.

A typical procedure for obtaining $Zr(HPO_4)_2 \cdot 0.5H_2O$ is the following: 2 g of ZrO_2 are added to a solution com-

0022-4596/94 $6.00
Copyright © 1994 by Academic Press, Inc.
All rights of reproduction in any form reserved.

posed of 30 ml of 14.8 *M* H_3PO_4 and 2.56 g of P_4O_{10} in a Pyrex vessel. The vessel is sealed and then shaken for 10 min; finally, the vessel is put into a steel container and placed in a 230°C oven for 48 hr with shaking. After rapid cooling to room temperature, the solid is separated from the mother liquor by centrifugation, washed with deionized water, and stored over P_4O_{10}. The value of interlayer spacing of the compound is independent of storage time.

Analytical Procedures

Quantitative analyses of Zr and phosphate groups were performed according to the procedures described in (16).

Coupled TG-DTA curves were taken with a Stanton STA781 thermoanalyzer at a heating rate of 5°C/min in flowing air. X-ray diffraction (XRD) patterns were recorded at room temperature on a computer-controlled Philips diffractometer equipped with a pulse-height analyzer; Ni-filtered Cu$K\alpha$ radiation (λ = 1.54178 Å) was used. Side-loading of the sample was used for data collection to minimize preferred-orientation phenomena. Data collection at 100°C was performed on a Siemens D-500 diffractometer equipped with an E. Bühler HDK 2.3 high temperature attachment. Densities were determined picnometerically using CCl_4 as the moving liquid. The ion exchange experiments were performed by titrating 300 mg of the sample suspended in 30 ml 0.1 *M* NaCl solution with 0.1 *M* NaOH solution, under nitrogen; a Mettler DL 40 automatic titrator operating in the equilibrium point mode was used.

Structural Analysis

XRD patterns were indexed on the basis of a monoclinic unit cell by the aid of the computer program TREOR (17).

Systematic absences in the XRD pattern indicated *C*2/*c* or *Cc* as possible space groups. The centrosymmetric space group *C*2/*c* was initially assumed and successively confirmed by the refinement.

Thirty-six unambiguously indexed reflections were selected in the XRD pattern and their intensities were determined by the aid of the deconvolution routine FIT (package DIFFRAC, from Siemens). Starting from this set of reflections, after correction for Lp and multiplicity, a Patterson map was calculated, which allowed Zr and P atoms to be located. Approximate location of oxygens atoms was obtained by difference Fourier maps.

Structure refinement was performed by the full-profile fitting method (Rietveld analysis (18)), by using a modified version (19) of the computer program PREFIN (20). The pseudo-Voigt profile function, with a refinable Gaussian contribution, was used. The refinement was performed by considering the contribution of both $K\alpha 1$ and $K\alpha 2$ radiation (2 : 1 intensity ratio) to the reflection profile. An angular dependence of the peak full-width at half maximum (FWHM) was assumed according to the Caglioti–Paoletti–Ricci equation (21). Reflection intensities were distributed over five FWHMs on either side of the peak maximum. Due to the high peak asymmetry, the (002) reflection was excluded from the refinement. Contrary to other similar materials (19, 22), no significant anisotropic line-broadening effects, due to different crystallite size along the unit cell vectors, were observed. The background contribution was defined by linear interpolation of the intensity measured in a region free of Bragg peaks. Neutral atomic scattering factors were from Cromer and Mann (23). A rigid HPO_4 group was considered by assuming the geometry reported for α-$Zr(HPO_4)_2 \cdot H_2O$ (25). Water oxygen was located on the two-fold axis (0, *y*, 1/4) with the *y* value adjusted in such a way that the distance from the pendant OH group is 2.8 Å (hydrogen bond distance). Refinement involved both nonstructural (scale factor, 2θ zero point, background intensities, FWHM coefficients, and Gaussian contribution to the pseudo-Voigt function) and structural parameters (unit cell dimensions, atomic coordinates, and isotropic thermal parameters for Zr and P). In the final step, individual atomic positions were refined. Iteration was stopped when the ratio shift/standard deviation for all the parameters was less than unity.

RESULTS AND DISCUSSION

In order to have a screening of the possible phases obtainable in the system Zr(IV)-H_3PO_4, preliminary experiments were carried out varying some of the synthesis parameters. In particular, the temperature was varied from 200 to 250°C, the time of reaction from 12 to 64 hr and the concentration of phosphoric acid from 15.5 to 17 *M*. In the earlier experiments both ZrO_2 and α-$Zr(HPO_4)_2 \cdot H_2O$ were used as the source of zirconium, but no differences in the final products were found. It was therefore decided to use ZrO_2, in the H_3PO_4/ZrO_2 ratio of 30 for the subsequent syntheses. Both the H_3PO_4 concentration and the reaction time were found to affect the extent of hydration in the crystallized phases.

An anhydrous zirconium phosphate, quite similar to that already described by Clearfield and named ε-$Zr(HPO_4)_2$ (13), was observed after 24 hr when a 17.0 *M* H_3PO_4 concentration and temperatures in the range 200–230°C were used. After 60 hr, complete conversion to cubic ZrP_2O_7 was obtained.

At lower H_3PO_4 concentrations (15.5–16.0 *M*) a different phase, with an interlayer distance of 7.42 Å, was initially formed. This phase, not previously described in the literature, was identified as a hemihydrate form of α-zirconium phosphate. After 60 hr ZrP_2O_7 was again the only phase detected. At a higher reaction temperature, conversion of both the anhydrous and the hemihydrate

phases to pyrophosphate occurs faster, the latter being the only phase observed by operating over 250°C. A typical procedure for the preparation of α-$Zr(HPO_4)_2 \cdot 0.5H_2O$ is reported under Experimental.

It should be noted that Clearfield *et al.* reported the preparation of a hemihydrate form of $Zr(HPO_4)_2$ with an interlayer distance of 7.15 Å (13). The X-ray pattern of this phase, named by the authors δ-ZrP, as well as the reported thermal and ion exchange behavior, differs remarkably from those of the hemihydrate phase of the present study.

Physicochemical and Structural Characterization

A well-crystallized product with composition $Zr(HPO_4)_2 \cdot 0.5H_2O$ was obtained by the above-mentioned procedure. Thermogravimetric analysis of the product indicated a total weight loss of 9.1%, corresponding to 1.5 mole of H_2O per mole of Zr (Fig. 1); 0.5 moles of water, lost between 180 and 550°C, were ascribed to crystallization water. The remaining mole of water, lost between 550 and 750°C, derives from the condensation of (HPO_4) to (P_2O_7) groups. As a matter of fact, the sample was found to be completely converted into ZrP_2O_7 at the end of the TGA run.

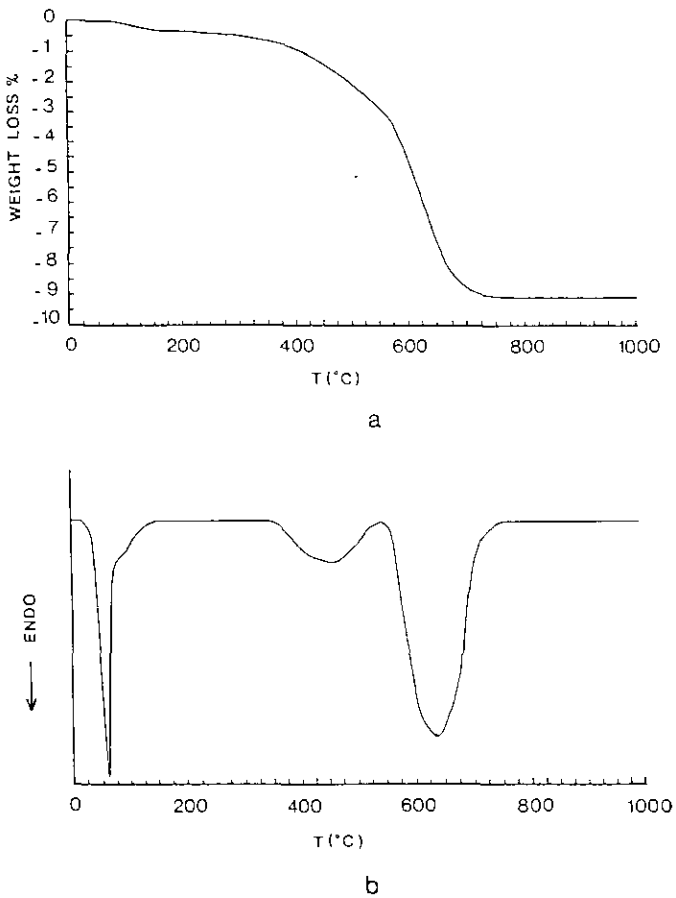

FIG. 1. TG(a) and DTA (b) curves of α-$Zr(HPO_4)_2 \cdot 0.5H_2O$.

TABLE 1
Crystallographic Data

T(°C)	25	100
Formula	$Zr(HPO_4)_2 \cdot 0.5H_2O$	$Zr(HPO_4)_2 \cdot 0.5H_2O$
Mw	292.19	292.19
Crystal system	Monoclinic	Trigonal
Space group	$C2/c$	$R\bar{3}$
Z	4	3
Dcalc (Mg/m^3)	2.685	2.647
Dexp (Mg/m^3)	2.70	n.d.
F(000)	564	423
μ(Cu$K\alpha$) (cm^{-1})	172.4	170.0
λ (Cu$K\alpha$) (Å)	1.54178	1.54178
a (Å)	9.1478(5)	5.3743(5)
b (Å)	5.3242(3)	—
c (Å)	15.288(1)	21.982(2)
β (°)	103.848(6)	—
V (Å^3)	722.9(1)	549.8(2)
Cross-section (Å^2)[a]	23.64	25.01
2θ range (°)	15–72	10–67
Step size (°2θ)	0.03	0.03
Counting time (s/step)	20	3
No. of steps	1901	1901
No. of reflections	173	52
No. of variables	27	22
No. of atoms	7	5
R_p[b]	0.079	0.087
R_{wp}[c]	0.102	0.124
R_2'[d]	0.132	0.148

[a] 23.91 Å^2 in α-$Zr(HPO_4)_2 \cdot H_2O$ (24).
[b] $R_p = \Sigma |I_{obs} - I_{calc}| / \Sigma |I_{obs}|$.
[c] $R_{wp} = \sqrt{[\Sigma w_i (I_{obs} - I_{calc})^2 / \Sigma w_i I_{obs}^2]}$.
[d] $R_2' = \Sigma |I_{obs} - I_{calc}| / |I_{obs} - I_{bkg}|$.

The product crystallizes in the form of hexagonal platelets, with an average diameter of about 4 μm (Fig. 2). The ratio ((mass density × interlayer distance)/(formula weight)), which is known to depend on the layer-type structure (24) (6.8×10^{-10} and 9.3×10^{-10} mole · cm^{-2} for α- and γ-type, respectively), was calculated by considering the mass density, 2.70 g · cm^{-3}, and the value of the interlayer distance, 7.42 Å (from d(002)). The resulting value of 6.86×10^{-10} mole · cm^{-2} is strongly indicative of an α-type layer structure.

The least-squares structure refinement, performed as described in the Experimental section, led to a good fit of the experimental XRD pattern (Fig. 3). Table 1 lists the final disagreement factors together with the main crystallographic data. Atomic parameters and the main geometrical features are reported in Table 2 and the structure is represented in Fig. 4. Geometry of the $[ZrO_6]$ octahedron and of the phosphate group are similar to those observed in α-$Zr(HPO_4)_2 \cdot H_2O$ (25), while the mean value of the Zr–O–P angle (158°) is significantly larger than

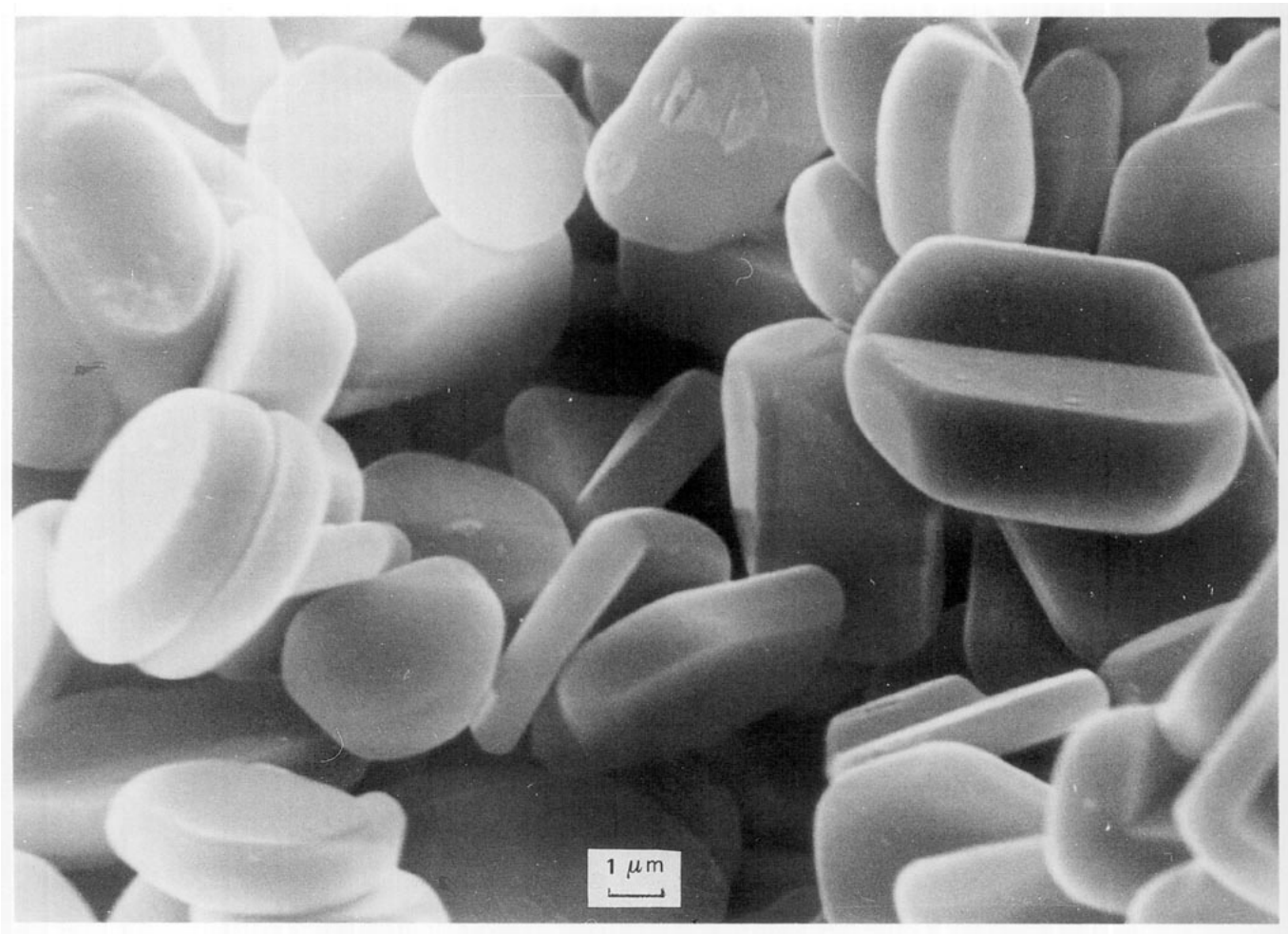

FIG. 2. SEM micrograph of α-$Zr(HPO_4)_2 \cdot 0.5H_2O$.

the corresponding value found in the monohydrate phase (150.8°). In spite of that, the cross-section, namely, the free area associated to every OH group on the layer plane, which depends on the Zr–O–P angle (22), slightly decreases (Table 1). This may be due to the lower mean Zr–O bond distance with respect to that found in the monohydrate phase (2.033 and 2.064 Å, respectively).

Unlike α-$Zr(HPO_4)_2 \cdot H_2O$, in which only intralayer hydrogen bonds are present (25), crystallization water forms interlayer hydrogen bonds (HO···Ow distances, 2.88(2) and 2.92(2) Å). This feature accounts for the different behaviors of the hemihydrate and monohydrate forms of zirconium phosphate, i.e., (a) the formation of a poorly crystallized anhydrous $Zr(HPO_4)_2$ phase (d = 7.45 Å) upon thermal treatment of the hemihydrate; (b) the impossibility of converting the hemihydrate into the monohydrate, even after refluxing for a long time in water.

Figure 5 shows the potentiometric titration curve with an NaOH solution. The exchange process occurs in two steps. The first, at pH 2.8, corresponds to 50% exchange ($Zr(NaPO_4)(HPO_4) \cdot 5H_2O$, interlayer spacing d = 11.9 Å), the second, at pH 6.2, to the fully exchanged phase ($Zr(NaPO_4)_2 \cdot 3H_2O$, d = 9.9 Å). This behavior is similar to that observed for the monohydrate phase (26). $Zr(HPO_4)_2 \cdot 0.5H_2O$ cannot be regenerated from the sodium salts, with the elution of $Zr(NaPO_4)_2 \cdot 3H_2O$ with 0.1 M HCl leading to $Zr(HPO_4)_2 \cdot H_2O$.

High-Temperature Study

DTA analysis of $Zr(HPO_4) \cdot 0.5H_2O$ (Fig. 1) shows (besides the two broad endotherms related to the above-mentioned water losses) a sharp endotherm at about 70°C (ΔH = 3.21 kJ/mole), with no associated weight loss in the TGA curve. The transition was found to be completely reversible. XRD analysis showed that the above-mentioned endotherm is related to the transition from the monoclinic phase to a trigonal phase, accompanied by a

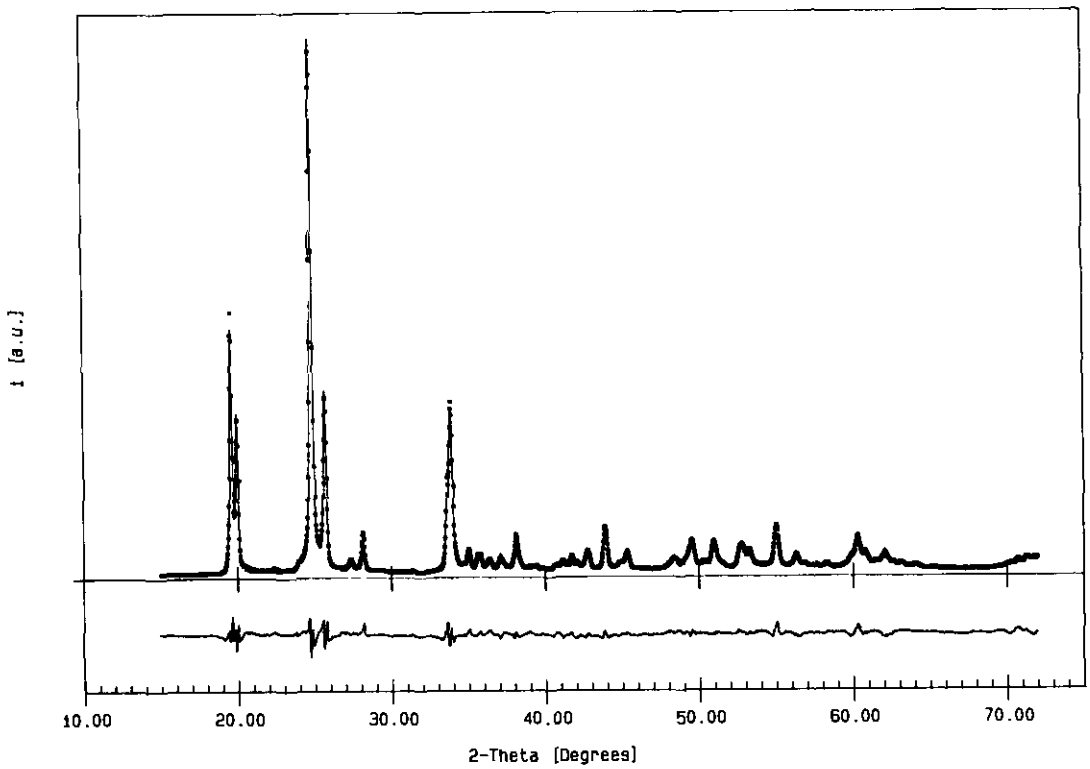

FIG. 3. Experimental (•), calculated (—), and difference (lower) profiles for the room-temperature form of α-$Zr(HPO_4)_2 \cdot 0.5H_2O$.

slight reduction of the interlayer distance to 7.33 Å. The XRD pattern recorded at 100°C was fully indexed with a trigonal unit cell. Systematic absences and chemical considerations suggested $R\bar{3}$ as the possible space group. As a starting set for Rietveld analysis, the Zr atom was placed on $\bar{3}$ (0, 0, 0), P and O(H) on 3 (1/3, 2/3, z, with

TABLE 2
Atomic Parameters and Main Geometrical Data for α-$Zr(HPO_4)_2 \cdot 0.5H_2O$ at 25°C

Atom	x	y	z	B_{iso} (Å^2)
Zr	1/4	1/4	1/2	1.08(9)
P	0.3673(5)	0.749(2)	0.3884(3)	1.5(2)
O(1)	0.5355(5)	0.787(4)	0.4181(7)	2.5
O(2)	0.318(2)	0.501(3)	0.420(1)	2.5
O(3)	0.285(2)	0.969(3)	0.419(1)	2.5
O(4)	0.320(1)	0.728(5)	0.2833(3)	2.5
O(w)[a]	0	0.654(3)	1/4	2.5

Zr–O(1)	2.07(1) Å	Zr–O(1)–P	159.2(12)°
Zr–O(2)	2.01(2) Å	Zr–O(2)–P	158.0(12)°
Zr–O(3)	2.02(2) Å	Zr–O(3)–P	156.9(12)°
P–O(1)	1.51(1) Å	O(1)–P–O(2)	112.4(9)°
P–O(2)	1.51(2) Å	O(1)–P–O(3)	110.5(8)°
P–O(3)	1.52(2) Å	O(1)–P–O(4)	109.1(8)°
P–O(4)	1.56(1) Å	O(2)–P–O(3)	111.4(9)°
O(w)···O(4)	2.88(2) Å	O(2)–P–O(4)	103.5(9)°
O(w)···O(4′)	2.92(2) Å	O(3)–P–O(4)	109.6(8)°

Note. ESDs are given in parentheses.
[a] Water oxygen, occupancy 0.5, not refined.

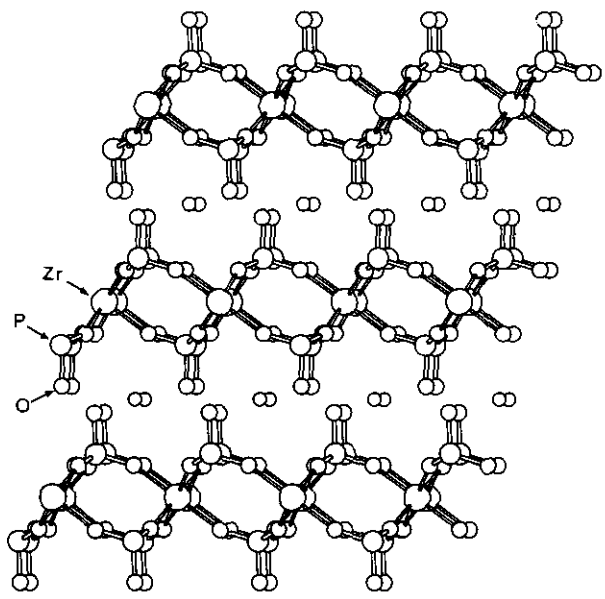

FIG. 4. Schematic drawing of the structure of the room-temperature form of α-$Zr(HPO_4)_2 \cdot 0.5H_2O$.

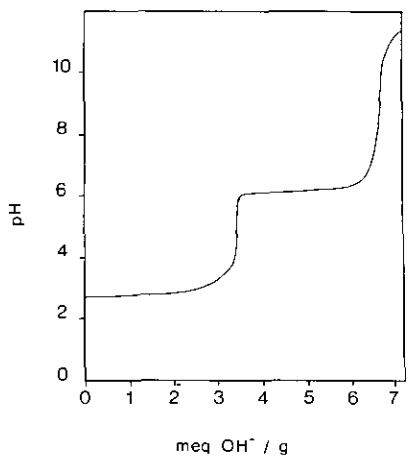

FIG. 5. Potentiometric titration curve of α-$Zr(HPO_4)_2 \cdot 0.5H_2O$ with NaOH 0.1 *M* in the presence of 0.1 *M* added NaCl. Experimental conditions: solid/liquid ratio = 1 g/100 ml.

TABLE 3
Atomic Parameters and Main Geometrical Data for α-$Zr(HPO_4)_2 \cdot 0.5H_2O$ at 100°C

Atom	*x*	*y*	*z*	B_{iso} (Å^2)
Zr	0	0	0	1.3(2)
P	1/3	2/3	−0.0732(4)	1.9(2)
O(1)	1/3	2/3	−0.1442(7)	3.0
O(2)	0.177(4)	0.353(4)	−0.0556(7)	3.0
O(*w*)[a]	0	0	1/2	3.0

Zr–O	6 × 2.05(2) Å	Zr–O(2)–P	158.2(13)°
P–O(1)	1.56(2) Å	O(1)–P–O(2)	104.9(9)°
P–O(2)	3 × 1.51(2) Å	O(2)–P–O(2)	113.4(11)°
O(*w*)···O(1)	3.14(1) Å		

Note ESDs are given in parentheses.
[a] Water oxygen, occupancy 0.5, not refined.

P–O(H) distance of 1.56 Å), and O in a general position. Water oxygen was located on $\bar{3}$ (0, 0, 1/2) with 0.5 occupancy. Refinement was performed as previously described for the room-temperature phase, leading to a satisfactory fit of the experimental pattern (Fig. 6). Those regions of the pattern containing contributions from Ta (sample holder) were excluded from the refinement. Crystallographic data are reported in Table 1; final atomic coordinates and the main geometrical features are listed in Table 3. The refined structure (Fig. 7) confirms the structural model adopted and consists of a stack of α-type layers shifted with respect to each other by 2/3*a* and 1/3*b*, producing a sequence of the *ABC* type. The water molecules are located exactly at the center of four OH

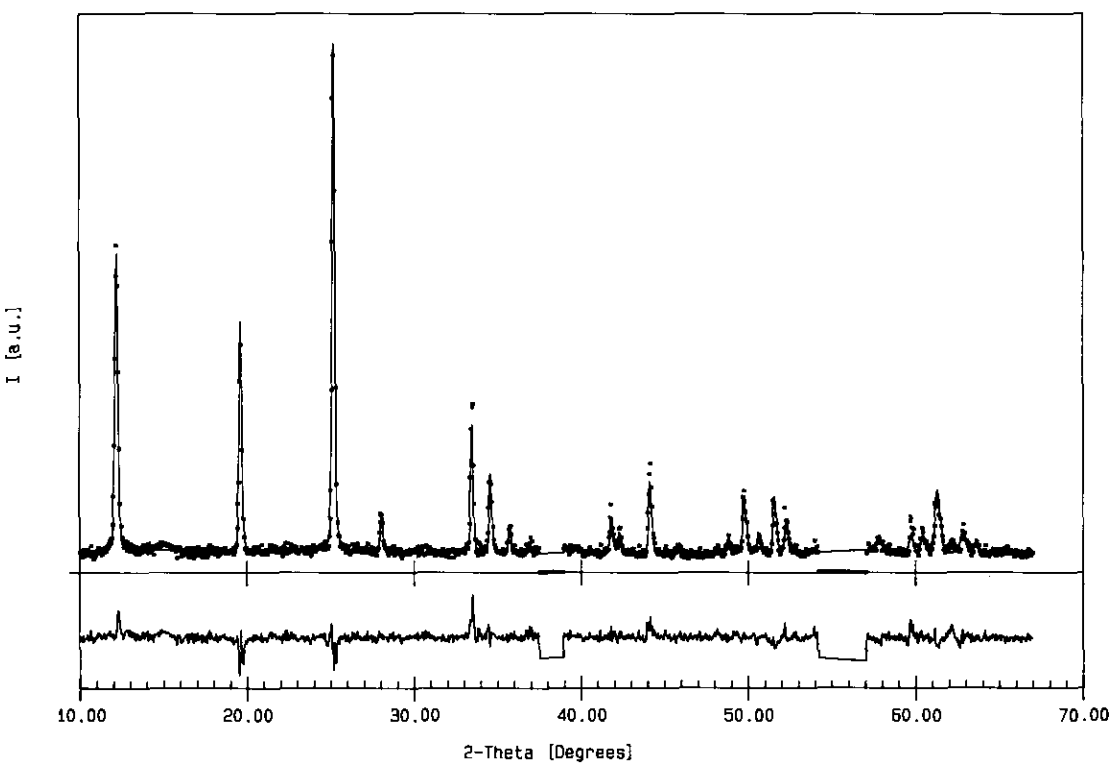

FIG. 6. Experimental (•), calculated (—) and difference (lower) profiles for the high-temperature form of α-$Zr(HPO_4)_2 \cdot 0.5H_2O$.

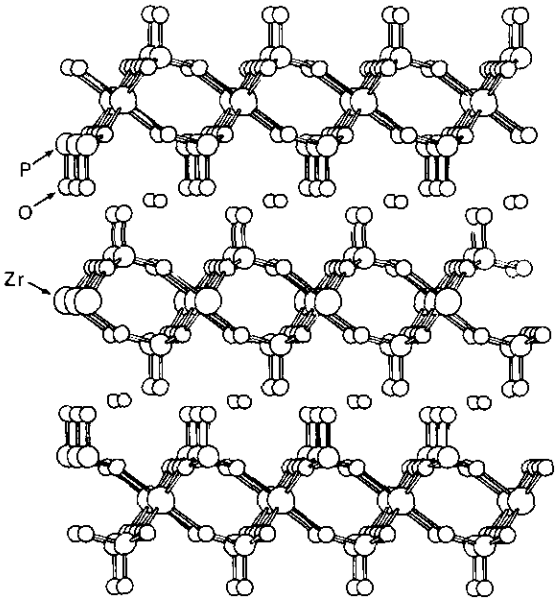

FIG. 7. Schematic drawing of the structure of the high-temperature form of α-$Zr(HPO_4)_2 \cdot 0.5H_2O$.

groups belonging to adjacent layers. The HO···Ow distance, 3.14(1) Å, is rather long and may indicate the formation of very weak hydrogen bonds.

In reality, water molecules might be randomly distributed on each side of the layer, with the formation of intralayer hydrogen bonds. In this case, the location of the water on (0, 0, 1/2) has to be considered as an average of the two possible positions. However, no definite information is obtainable from the XRD data.

A systematic study on the thermally induced phase transitions of layered zirconium phosphates (27) has shown that a trigonal phase with similar unit cell parameters is obtained when α-$Zr(HPO_4)_2 \cdot H_2O$ microcrystals are quickly heated to 250°C without an appreciable loss of crystallization water. The same study (to be published elsewhere) did not provide any evidence of the formation of the hemihydrate from partial dehydration of the monohydrate phase.

REFERENCES

1. A. Clearfield and J. A. Stynes, *J. Inorg. Nucl. Chem.* **26,** 117 (1964).
2. G. Alberti and E. Torracca, *J. Inorg. Nucl. Chem.* **30,** 317 (1968).
3. A. Clearfield, R. H. Blessing, and J. A. Stynes, *J. Inorg. Nucl. Chem.* **30,** 2249 (1968).
4. A. Clearfield and G. D. Smith, *Inorg. Chem.* **8,** 431 (1969).
5. A. N. Christensen, E. K. Andersen, I. G. K. Andresen, G. Alberti, M. Nielsen, and M. S. Lehemann, *Acta Chem. Scand.* **44,** 865 (1990).
6. G. Alberti, U. Costantino, A. Allulli, and N. Tomassini, *J. Inorg. Nucl. Chem.* **40,** 1113 (1978).
7. G. Alberti, R. K. Biswas, S. Murcia Mascarós, and R. Vivani, *React. Polym.* **19,** 1 (1993).
8. A. Clearfield (Ed.), "Inorganic Ion Exchange Materials," Chap. I, II, and III and references therein. CRC Press, Boca Raton, FL, 1982.
9. G. Alberti, *Acc. Chem. Res.* **11,** 163 (1978).
10. G. Alberti and U. Costantino *in* "Intercalation Chemistry" (M. S. Whittingham and A. J. Jacobson, Eds.), pp. 147–180. Academic Press, New York, 1982.
11. G. Alberti and U. Costantino *in* "Inclusion Compounds" (J.L. Atwood, J.E.D. Davies, and D.D. MacNicol, Eds.), Chap. 5. Oxford Univ. Press, London, 1991.
12. A. Clearfield, *Comments Inorg. Chem.* **10**(283), 89 (1990).
13. A. Clearfield, A. L. Landis, A. S. Messina, and J. M. Troup, *J. Inorg. Nucl. Chem.* **35,** 1099 (1973).
14. A. Clearfield and J. R. Thomas, *Inorg. Nucl. Chem. Lett.* **5,** 775 (1969).
15. E. Torracca, G. Alberti, R. Platana, P. Scala, and P. Galli, *in* "Ion Exchange in the Process Industry." Proceedings of the Society of Chemical Industry Meeting, London, July 16–18, 1969.
16. G. Alberti, A. Conte, and E. Torracca, *J. Inorg. Nucl. Chem.* **28,** 225 (1966).
17. P. E. Werner, L. Eriksson, and M. Westdahl, *J. Appl. Crystallogr.* **18,** 65 (1985).
18. H. M. Rietveld, *Acta Crystallogr.* **22** 151 (1967); *J. Appl. Crystallogr.* **2,** 65 (1969).
19. R. Millini, G. Perego, and S. Brückner, *Mater. Sci. Forum* **79/82,** 239 (1981).
20. A. Immirzi, *Acta Crystallogr. Sect. B* **36,** 2378 (1980).
21. G. Caglioti, A. Paoletti, and F. P. Ricci, *Nucl. Instrum.* **3,** 223 (1958).
22. R. Millini, G. Perego, U. Costantino, and F. Marmottini, *Microporous Mater.*, **2,** 41 (1994).
23. D. T. Cromer and B. Mann, *Acta Crystallogr. Sect. A* **24,** 321 (1968).
24. G. Alberti, U. Costantino, and M. L. Luciani Giovagnotti, *J. Inorg. Nucl. Chem.* **41,** 643 (1979).
25. J. M. Troup and A. Clearfield, *Inorg. Chem.* **16,** 3311 (1977).
26. A. Clearfield, W. L. Duax, A. S. Medina, G. D. Smith, and J. R. Thomas, *J. Phys. Chem.* **73,** 3424 (1969).
27. G. Alberti, U. Costantino, R. Millini, G. Perego, and R. Vivani, to appear.